

Influences of liquid electrolyte and polyimide identity on the structure and conductivity of polyimide–poly(ethylene glycol) materials

Elyse Coletta,¹ Michael F. Toney,² Curtis W. Frank¹

¹Department of Chemical Engineering, Stanford University, Stanford, California, 94305

²Stanford Synchrotron Radiation Lightsource, Menlo Park, California 94025

Correspondence to: E. Coletta (E-mail: elyse.coletta@gmail.com)

ABSTRACT: Current fuel cell technology demands improvements for widespread use, and novel polymer materials may be able to achieve the necessary enhancements. This work inspects the composition, structure, and properties of poly(ethylene glycol) (PEG)–aromatic polyimide systems aimed at polymer electrolyte membrane applications, as PEG is a known ion conductor and aromatic polyimides are quite stable. Liquid electrolytes were incorporated into the polymers through soaking to achieve ionic conductivity. By varying polyimide and liquid electrolyte, the polymers were analyzed for their structure and conductivity. Fourier transform infrared spectroscopy, thermal gravimetric analysis, differential scanning calorimetry, small-angle X-ray scattering, electrochemical impedance spectroscopy, and cyclic voltammetry were used as characterization tools. Electrolyte identity impacts liquid uptake and conductivity. Polyimide identity can influence the size and variability of the doped polymer structure, which ultimately can change conductivity by up to 28%, with the maximum conductivity being 102 mS/cm at 80°C and 70% RH. © 2014 Wiley Periodicals, Inc. *J. Appl. Polym. Sci.* 2015, 132, 41675.

KEYWORDS: copolymers; ionic liquids; membranes; nanostructured polymers; structure–property relations

Received 2 August 2014; accepted 30 October 2014

DOI: 10.1002/app.41675

INTRODUCTION

The need for additional energy sources is paramount for current and future standards of living. More sustainable and clean energy sources can be found in a variety of applications including nuclear, hydroelectric, geothermal, solar, wind, and hydrogen. Because of the respective limitations and disadvantages of each type of energy source, multiple technologies will likely be needed to help convert cleaner, more sustainable energy to meet the global demand. Also, because of the intermittency of some of the newer energy sources, such as wind and solar, the need for energy storage devices is also important. Fuel cells represent devices that can be used both for energy conversion and energy storage. Polymer electrolyte membrane fuel cells (PEMFCs) are of particular interest because they have high achievable power densities and can function well in portable applications because of their operating temperature window and easier assembly than some other fuel cell types. Despite the advantages of PEMFCs, there are still technological challenges to overcome before these devices can be generally practical. In particular, PEMFCs are limited to low operating temperatures in high humidity environments owing to the current PEMs.¹

The industry objective is to move toward a PEM that can function in a wider range of operating conditions. The optimal mem-

brane is one that can operate at higher temperatures and lower humidity conditions than current membranes while still maintaining the other properties needed for an effective PEM. The challenging aspect of PEM design is that the membrane requires a variety of different properties in order to function well. High-quality PEMs need to be thermally, mechanically, and electrochemically stable as well as have high, selective conductivity for protons as opposed to electrons in addition to achieving a minimal permeability to fuel gases.¹ The reality is that even though much research has been performed previously in the field of PEMs there is still much improvement that needs to be made in order to make these devices a solution for meeting future energy and environmental demands.

The objective becomes how these polymer materials can be engineered to achieve the optimal properties desired in a PEM. This work aims at expanding the insight of how material identity can impact the nanometer-level structure and conductivity of the polymer system through assessing variations in polymer and liquid electrolyte identity. The PEM community has learned from Nafion that polymer–liquid interactions can impact structure and conductivity. Ionic liquids have been incorporated into Nafion previously, for example, and these studies have shown that more hydrophilic ionic liquids can enhance the connectivity of the

ionic domains, whereas more hydrophobic ionic liquid incorporation can result in higher uptake into the polymer, but may also result in a collapse of the ionic domains.^{2–4} This work aims at expanding the knowledge of polymer–liquid interactions by analyzing various poly(ethylene glycol) (PEG)–aromatic polyimide (PI) membranes doped with different protic liquids.

Aromatic polyimides in the current materials function as the mechanical matrix for the membrane and have been shown to exhibit a wide variety of behaviors. Polyimides, both with and without PEG, have been studied previously and have been found to exhibit differences in structural order, interactions, and free volume, which can impact behavior and properties. These material variations can be achieved through the specific choice of aromatic monomers.^{5–15} In this work, protic liquids, including ionic liquids, have been incorporated into some of the polymer membranes in order to provide the ion conduction capability, both the membrane ion source and vehicle, so polymer–ionic liquid interactions are expected to influence performance.

The field of ionic liquids is broad, largely because ionic liquids have low vapor pressure and good electrochemical stability, which are advantageous properties in a variety of applications.^{2,3} Ionic liquids are also attractive because they have ionic behavior but possibly different pH levels compared with traditional ionic solutions.¹⁶ A wide range of ionic liquids have been doped in numerous polymers for polymer electrolyte and sensor applications. Some specific polymers that have been doped with ionic liquids for various applications include: sulfonated poly(ether ketone),^{17,18} polyurethane,¹⁹ poly(propylene carbonate),^{20–23} poly(vinyl acetate),²⁴ poly(vinyl chloride), cellulose triacetate,²⁵ poly(styrene-*b*-methyl methacrylate), poly(styrene-*b*-methyl methacrylate),²⁶ poly(styrene-*b*-methylbutylene),²⁷ poly(styrene-*b*-2-vinylpyridine),^{28,29} polybutadiene,³⁰ poly(vinylidene fluoride),³¹ poly(vinylidene fluoride-*co*-hexafluoropropylene),^{32–41} polytetrafluoroethylene, polyethylene,⁴² poly(methyl methacrylate),^{43,44} poly(vinyl pyridine),^{45,46} poly(ethyleneimine),⁴⁷ poly(diallyldimethylammonium chloride), poly(allylamine hydrochloride), poly(*n*-isopropylacrylamide),^{48–51} polysulfides,⁵² polysulfone,⁵³ and polyimides.^{54–58} A large portion of the work involving ionic liquids in PEMs has involved the use of ionic liquids as anhydrous ion vehicles.^{17,18,20,21,23,47,54,59–72} Ideally, with little to no water content, these PEMs will be able to function at moderate to high temperatures and at lower humidity levels than current PEMs.

The interaction of ionic liquids and polymers is complex and a variety of results have been obtained.^{2,3} Ionic liquids can impact the thermal transitions of a polymer, level of crystallinity, phase separation, and chain mobility. Previous studies of polymer–ionic liquid systems for electrolyte applications have shown that solvation dynamics, strength of ionic interaction, and polymer relaxation motions all influence conductivity. For example, ionic liquids have been shown to act as plasticizing agents for polymers, which enhance polymer chain mobility and membrane ionic transport. Some ionic liquids contain one or two bulky, flexible ions that aid in enhancing the conductivity by increasing free volume and inhibiting crystallinity. To a certain extent,

the more ionic liquid that can be incorporated into a polymer, the higher the conductivity. The higher ionic liquid content inhibits polymer crystallinity and can increase the ionic concentration and the vehicle concentration. However, at some point, increasing the ionic liquid content can decrease the mechanical integrity of the PEM.^{2,3,73,74} In addition to the polymer behavior being influenced by the ionic liquid, the liquid behavior can also be impacted by the presence of polymer. Data from previous work suggest that the conductivity of an ionic liquid–polymer system is not always correlated with the natural properties of the ionic liquid alone.^{2,3} Confinement of ionic liquids in polymer matrices can cause changes in local concentration, hydrogen bond structure, and frustration of Van der Waals forces, which could change the conductivity.

Other insights can be gained from studies in which various ionic liquids were doped into block copolymers, including polystyrene–poly(ethylene oxide), polystyrenesulfonate–poly(methylbutylene), polystyrene–poly(methyl methacrylate), and polyisoprene–polystyrene–poly(ethylene oxide).^{4,26,27} Incorporation of ionic liquids is expected to change the χ parameter, volume, segmental motion, chain conformation, and dielectric constant. These changes can then manifest in terms of variations in polymer domain size, polymer phase domain boundary clarity, and anisotropy of structure. Doping of ionic liquids can also cause disorder-to-order transitions as well as transitions from one morphological state to another. The nature of the changes is determined by the polymer and ionic liquid identities, the amount of ionic liquid, and preferential interaction of the ionic liquid of one polymer phase over the others.^{4,26,27,75}

In addition to generally understanding what can happen when ionic liquids and polymers interact, the interaction of ionic liquids in PEG-containing polymer systems is very relevant to the current work. Studies have shown that ionic liquids can enhance the phase segregation in PEG-containing systems, specifically block copolymers of poly(ethylene oxide-*b*-styrene), because of selective association of the ionic liquid with the poly(ethylene oxide) over the polystyrene.^{2,3} The heightened phase separation further decouples the mechanically strong polymer portion from the conducting phase, creates regions of more concentrated ionic liquid, and causes changes in structure.

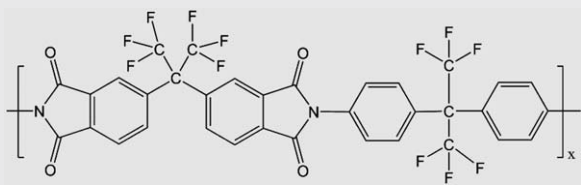
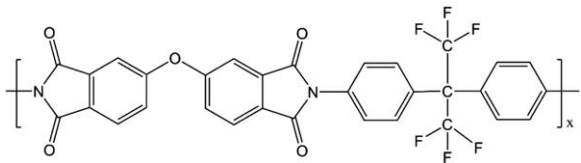
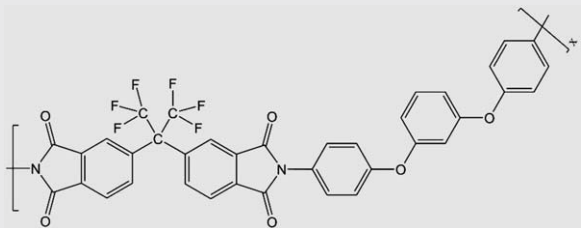
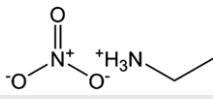
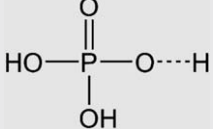
While both PEG and polyimides have previously been combined with ionic liquids, most of the studies involve different polymer combinations or configurations compared with this work. In addition, relatively few studies focus on both structure and conductivity and most that do tend to examine block copolymers. In this work, insight can be gained into the relationship between composition, structure, and conductivity of random copolymers.

EXPERIMENTAL

Materials

4,4'-(1,3-Phenylenedioxy)dianiline (PDODA), 4,4'-(hexafluoroisopropylidene)diphthalic anhydride (6FDA), poly(ethylene glycol) bis(3-aminopropyl) terminated (M_n 1500), and *N,N*-dimethylacetamide (DMAc) were purchased from Sigma Aldrich and used as received. 4,4'-Oxydiphthalic anhydride (ODPA) and 2,2-bis(4-aminophenyl)hexafluoropropane (AP6F) were purchased from

Table I. Chemical Structures of the Synthesized Polyimides and the Electrolytes with Their Corresponding Abbreviations

Chemical structure	Abbreviation
	6FDA-AP6F
	ODPA-AP6F
	6FDA-PDODA
	EAN
	H ₃ PO ₄

TCI America and used as received. Ethylammonium nitrate (EAN) was purchased from Iolitec and used as received. Teflon film was purchased from McMaster-Carr and used as received. A phosphoric acid solution (85%) was purchased from Malinkrodt and used as received.

Synthesis

First, the poly(ethylene glycol) bis(3-aminopropyl) terminated and the aromatic diamine, either AP6F or PDODA, were placed into a three-neck flask. Then, the solvent, DMAc, was placed into the flask. The contents were stirred under nitrogen and gently heated to $\sim 50^\circ\text{C}$ until all the solids were dissolved. The flask was then cooled to $\sim 30^\circ\text{C}$ and a stoichiometric amount of aromatic dianhydride, either ODPA or 6FDA, was added to the flask slowly and in solid form over a period of 30 min. The known total solids concentration was between 0.075 and 0.09 g/mL. The contents of the flask were stirred at room temperature under nitrogen for 24 h and were then collected for future use.

Casting/Imidization

The poly(amic acid) precursor solutions were poured into a Teflon-lined glass dish and thermally imidized in an oven using the following heating protocol: ramp from 20 to 90°C over a period of 2 h and 15 min, then ramp to 130°C over a period of 3 h, hold at 130°C for 11 h, ramp to 155°C over a period of 3 h,

hold at 155°C for 1 h, and cool to 25°C over a period of 4 h. The dry, free-standing films were then collected for future testing.

Electrolyte Incorporation

The imidized free-standing films were cut into appropriate sizes and placed into the liquid electrolyte of choice in a closed container at room temperature for 24 h and then removed immediately and tested as needed. Table I shows some of the key chemical structures of the polymers that were synthesized, the electrolytes, and their corresponding abbreviations that will be used in subsequent discussions.

Characterization

Fourier transform infrared spectroscopy (FTIR) measurements were performed at room temperature using a Nicolet 6700 FTIR. Sample preparation involved the use of potassium bromide pellets. FTIR was used to qualitatively confirm the success of the undoped polymer synthesis.

Thermal gravimetric analysis (TGA) was performed using a Mettler Toledo TGA/SDTA 851e. Film samples between 1 and 15 mg were loaded into aluminum pans for testing. The thermal protocol involved heating from 25 to 600°C at a rate of $10^\circ\text{C}/\text{min}$. TGA was used to quantitatively determine the thermal stability of the undoped polymers in terms of mass loss as a function of temperature.

Differential scanning calorimetry (DSC) was performed using a TA Instruments Q100. Film samples between 1 and 10 mg were loaded into aluminum pans for testing. The following thermal protocol was used: equilibrate at 20°C, ramp at 5°C/min up to 120°C, hold at 120°C for 2 min, ramp at 5°C/min to 20°C, hold at 20°C for 2 min, and then repeat the cycle two more times. DSC was used to qualitatively determine the undoped polymer morphology by detecting the presence or absence of calorimetric exotherms and endotherms.

Electrolyte uptake measurements were performed on a subset of the polymer materials. The undoped polymer was first weighed and then soaked in the electrolyte of choice, either EAN or a 20 vol % solution of phosphoric acid, for 24 h at room temperature. The liquid-soaked polymer was then dabbed dry and reweighed to determine the amount of electrolyte uptake. The values for the phosphoric acid solution electrolyte are based on single measurements and those values for the ionic liquid uptake are based on an average of three different measurements.

Conductivity measurements were performed using a BT 552 Bekktech conductivity analyzer and a Gamry Instruments Reference 600 Potentiostat/Galvanostat/ZRA via electrochemical impedance spectroscopy (EIS) and cyclic voltammetry (CV). The AC impedance was performed with an amplitude of 10 mV over a frequency range of 200,000–0.1 Hz, measuring six points per decade. CV was performed for five cycles over the voltage window of –0.1 to 0.1 V at a sweep rate of 25 mV/s with a step size of 2 mV and a maximum current range of 0.01 mA. Measurements were performed under nitrogen at 70% relative humidity between 40 and 80°C unless otherwise noted. An initial pretreatment at 60°C for 45 min at low humidity was used to improve probe-to-film contact and have some equilibration of the equipment to the humidity levels. The conductivity values represent an average over three different films tested on different days with error bars representing 1 SD above or below the average unless otherwise noted. The individual film measurement values were based on an average of six measurements per single temperature on the same film. EIS and CV techniques were used to quantitatively assess the total and electrical conductivity, respectively, of the doped polymer films.

Small-angle X-ray scattering (SAXS) was performed at beamline 1–4 at SLAC Synchrotron Radiation Laboratory (Stanford, CA). The wave length of the X-ray beam was 1.4884 Å. Detector calibration was done using silver behenate and chicken tendon. Data were averaged over space and slit correction was used via Igor Nika software or a similar macro. All data are background corrected and based on an average exposure time of 5 min. All SAXS measurements were performed at room temperature and ambient humidity unless otherwise specified. All membranes doped with electrolyte were first pretreated at 60°C for 45 min to mimic the pretreatment performed before the conductivity measurements.

SAXS detected structural features on the length scale over a range from about 0.5–80 nm. The specific sample analysis varied based on the particular material being considered. Various scattering models were used to extract phenomenological parameters. For example, the SAXS data in this work often

showed shoulders with regard to intensity as a function of q , and the correlation length model was used to extract information from these shoulders.⁷⁶ The correlation length model is encompassed by eqs. (1) and (2).

$$I(q) = \frac{c}{1 + (q\xi)^m} + B \quad (1)$$

$$m = \frac{1}{\nu} \quad (2)$$

In this model, the correlation length of the domains, ξ , can be determined as well as the fractal dimension, m , and the scaling exponent, ν , by allowing B and c to be constants and fitting the intensity, I , data as a function of scattering vector, q . The fractal dimension is based on polymer scaling behavior and can give insight into the state or shape of the polymer domains. A fractal dimension of 3, corresponding to a collapsed chain, was chosen to model the correlation length of the PEG domains in the undoped polymers because the PEG domains were thought to be in a collapsed chain state due to the suspected phase separation from the aromatic polyimide. A fractal dimension of 1.7 corresponding to a swollen chain was used to model the PEG domains in samples swollen in liquid electrolyte that possessed a clearly defined shoulder. Because the data only covered up to one order of magnitude in q , and because data over two orders of magnitude of q is optimal, m was fixed to try to get a more accurate correlation length value and to keep the treatment consistent for all samples.

For peaks with a clear maximum, the parameter of interest was q_{\max} . The broad peak model, which is based on the correlation length model and can be seen in eq. (3), was used to extract the position of the maximum q .⁷⁶

$$I(q) = \frac{c}{1 + (|q - q_{\max}| \xi)^m} + B \quad (3)$$

In this case, the only parameter of interest was q_{\max} . The fractal dimension was again fixed at a number that was thought to be appropriate to designate the structural entity being described by the SAXS peak. For example, a fractal dimension of 1, representing a rigid rod, was chosen for imide packing features because of the rigidity of the aromatic rings. An m of 1.7, representing a swollen chain, was chosen for features related to the ionic liquid-doped PEG phase. To estimate the imide features once disordered or convoluted, an m of 2 was used because it appeared to give the best fit to the data, given that the features were only weakly present and the data typically only spanned a small range of q values. The original imide features would be expected to be rigid and not swell much. Taking into account that the material is then swollen in an ionic liquid thus impacting the rigid features, an m of 2 representing a Gaussian chain is likely to represent the swelling expected in a swollen polymer environment, balanced with the rigidity of the chain. For all samples, the q_{\max} was then converted to a real space distance, d , assuming Bragg's law. If Bragg's law is combined with the definition of the scattering vector, then the relationship between distance and scattering vector can be seen in eq. (4).

$$d_{\max} = \frac{2\pi}{q_{\max}} \quad (4)$$

Because of the clarity of the amorphous halo features, the spacing values for the features were estimated based on Bragg's law

Table II. List of Materials, Key SAXS Structural Components, and Associated Information

Material	Feature code	Feature origin	ξ or d Value (nm)	q Value (nm^{-1})
ODPA-AP6F-ODPA-PEG1500 (50%)	S_{PEGOF}	Disordered PEG domains	0.9	~ 2
	P_{aOF}	Aromatic polyimide order (aromatic dianhydride repeat unit)	15.3	0.41
6FDA-AP6F-6FDA-PEG1500 (50%)	S_{PEGFF}	Disordered PEG domains	0.9	~ 2
ODPA-AP6F-ODPA-PEG1500 (50%) EAN	F_{aOF}	Aromatic polyimide order with IL interference	15.0 ^a	0.42
	P_{PEGILOF}	IL-doped PEG order (spacing of doped PEG domains)	11.6	0.54
6FDA-AP6F-6FDA-PEG1500 (50%) EAN	P_{PEGILFF}	IL-doped PEG order (spacing of doped PEG domains)	13.4	0.47
6FDA-PDODA-6FDA-PEG1500 (50%)	S_{PEGFO}	Disordered PEG domains	0.9	~ 2
	F_{aFO}	Aromatic polyimide order with PEG interference	2.2 ^a	2.9
6FDA-PDODA-6FDA-PEG1500 (50%) EAN	P_{PEGILFO}	IL-doped PEG order (spacing of doped PEG domains)	11.0	0.57

d Value corresponds to peaks and features. ξ value corresponds to shoulders.

^aEstimated spacing from a less-well-defined feature.

using the highest intensity measured from the scattering peak as the position of q_{max} .

For the purposes of quantifying differences in certain features, in some cases a full width half maximum (FWHM) was calculated. The FWHM is measured in terms of a q range and was calculated based on taking a half width half maximum directly from the SAXS data and assuming completely symmetric peaks for the sake of trying to avoid any impacts from convolution of multiple features or larger scale feature scattering.

The parameters that can be deduced from the SAXS data with some certainty include the presence of phase-separated domains, the spacing value of ordered domains, the approximate size of disordered domains, and the relative ordering of domains.

Parameters that can be indirectly deduced from the data include domain connectivity. Parameters that cannot be determined from the data include, but are not limited to, the shape of domains, the location of domains, the size of ordered domains, the spacing value of any disordered domains, and the amount of domain aggregation, phase separation, and domain ordering.

For the purposes of discussion, some of the key SAXS structural components are given code names with a P designation for peaks, S designation for shoulders, and F designation for more ambiguous features that either involve a very ill-defined peak with no clear maximum or a relatively narrow shoulder. A complete list of the features is listed in Table II. The shoulders typically represent randomly distributed PEG domains across all polyimide families and occur on similar length scales across materials. The peaks can correspond to aromatic polyimide

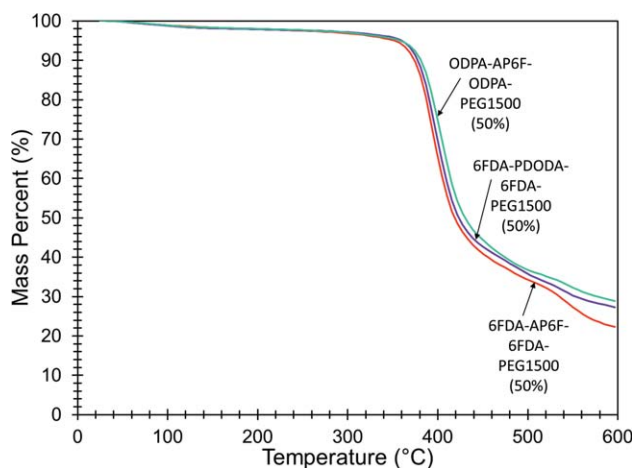


Figure 1. TGA curves of ODDA-AP6F-ODPA-PEG1500 (50%), 6FDA-PDODA-6FDA-PEG1500 (50%), and 6FDA-AP6F-6FDA-PEG1500 (50%). [Color figure can be viewed in the online issue, which is available at wileyonlinelibrary.com.]

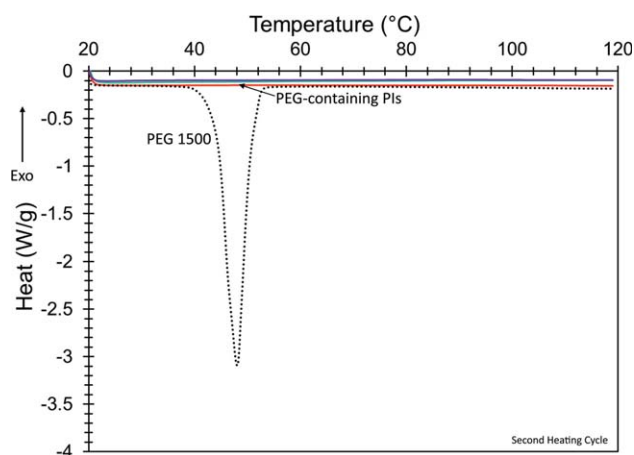


Figure 2. DSC curves of ODDA-AP6F-ODPA-PEG1500 (50%), 6FDA-PDODA-6FDA-PEG1500 (50%), and 6FDA-AP6F-6FDA-PEG1500 (50%). [Color figure can be viewed in the online issue, which is available at wileyonlinelibrary.com.]

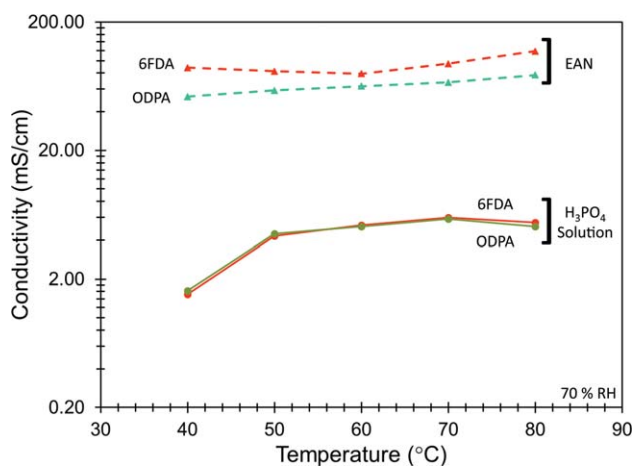


Figure 3. Conductivity of 6FDA-AP6F-6FDA-PEG1500 (50%) and ODPA-AP6F-ODPA-PEG1500 (50%) doped with phosphoric acid solution and EAN at 70% RH. [Color figure can be viewed in the online issue, which is available at wileyonlinelibrary.com.]

ordering and/or ionic liquid-doped PEG ordering depending on the specific material. The less-well-defined features correspond to aromatic polyimide order that has been impacted in some way by PEG and/or ionic liquid. The key features will be discussed in more detail in subsequent sections.

RESULTS AND DISCUSSION

Synthesis of Undoped Polymers

FTIR was first performed on the poly(amic acid) precursors and the final polymers in order to verify the success of the synthesis. The FTIR spectra of the polyimides include peaks indicating imidization.^{77–79} There was also a reduction in the features in the region related to the poly(amic acid).^{79,80} Through both the appearance of new absorption bands and the disappearance or loss of prominence of other bands, FTIR confirmed that the initial synthesis resulted in poly(amic acid) and that the final membranes were polyimides.

Thermal Stability of Undoped Polymers

The thermal stability of the undoped polymers in this analysis was tested to evaluate whether the polymers could survive over the intended operating temperature range of the fuel cell. The TGA results for these polymers can be seen in Figure 1. The thermal stability of the polymers was found to be sufficient for the fuel cell application operating conditions. There is no significant mass loss before 400°C for all the PEG-polyimide polymer systems tested. Specifically, there is <5% mass loss of the compounds for temperatures up to around 200°C, which is a more-than-adequate expected operating window for the fuel cell. The significant mass loss around 400°C is attributed to PEG degradation and occurs at a temperature similar to mass losses assigned to the PEG component in previously studied PEG-containing polyimides at around 250–450°C.^{5,11–15} The significant mass loss occurring around 550°C was attributed to the polyimide phase degradation and also occurs around the same temperature as mass losses that were assigned to the aromatic polyimide component in previously studied PEG-containing polyimides at around 450°C and higher.^{5,11–15} The thermal sta-

bility of the materials is similar across the different polyimide families.

Morphology of the Undoped Polymers

The morphology of the undoped polymers was also analyzed. The DSC results for the second heating cycle of the polymers of interest can be seen in Figure 2. The materials in Figure 2 are the same as in Figure 1 and include the following polyimide families: 6FDA-AP6F, 6FDA-PDODA, and ODPA-AP6F. The second heating cycle of the DSC data shows that the PEG-containing polyimides show a completely amorphous morphology with no evidence of crystallinity when compared with the PEG 1500 diamine reactant control by itself. The morphology does not change with a variation in the specific polyimide family.

The PEG chains are surrounded on each side by an aromatic repeating unit and are, thus, likely to be relatively isolated with large aromatic chain tethers on either end based on the chemistry scheme. The PEG is also expected to phase separate from the aromatic polyimide based on thermodynamic interactions of PEG with other hydrophobic materials as well as evidence of phase separation seen in previously studied PEG-containing polyimides.⁵ The existence of relatively short PEG segments whose mobility and configuration is impacted by surrounding material is expected to discourage PEG crystallization. In addition, similar PEG-containing polyimides with certain processing conditions have also shown no evidence of PEG crystallinity.^{13,81–84} Amorphous PEG morphology is advantageous for higher conductivity because the less tightly associated chains can associate with and transport ions in an easier fashion, as has been seen for past PEG electrolyte materials.^{85,86}

Conductivity of Polymers with Various Liquid Electrolytes

Initial attempts at creating PEMs involved soaking the polymers in a phosphoric acid solution. Success has been found in doping PBIs with phosphoric acid for PEM applications and, thus, phosphoric acid was the starting point for creating PEG-PI PEMs.^{87,88} However, the conductivity of those polymers doped with phosphoric acid solution was lower than desired. As a result, other types of liquid electrolyte dopants were also tried, with varying levels of success. The electrolyte resulting in membranes with the highest conductivity was EAN. The conductivity of the polymers doped with phosphoric acid solution when compared with the ionic liquid EAN measured at 70% RH,

Table III. Electrolyte Uptake Values for 6FDA-AP6F-6FDA-PEG1500 (50%) and ODPA-AP6F-ODPA-PEG1500 (50%) Doped with Phosphoric Acid Solution and EAN

Material	Electrolyte	Uptake (%)
6FDA-AP6F-6FDA-PEG1500 (50%)	H ₃ PO ₄ Solution	96
6FDA-AP6F-6FDA-PEG1500 (50%)	EAN	203
ODPA-AP6F-ODPA-PEG1500 (50%)	H ₃ PO ₄ Solution	73
ODPA-AP6F-ODPA-PEG1500 (50%)	EAN	149

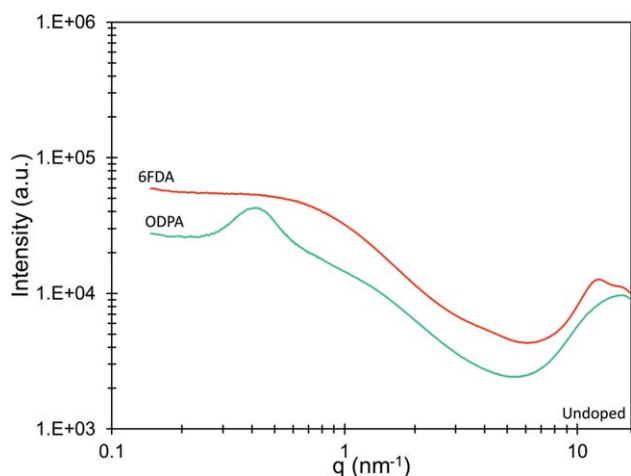


Figure 4. SAXS signatures of 6FDA-AP6F-6FDA-PEG1500 (50%) and ODP-AP6F-ODPA-PEG1500 (50%) polymers. [Color figure can be viewed in the online issue, which is available at wileyonlinelibrary.com.]

which include 6FDA-AP6F-6FDA-PEG1500 (50%) and ODP-AP6F-ODPA-PEG1500 (50%), can be seen in Figure 3. The conductivity data are based on single sample measurements of all the materials, but appear to be consistent across both of the materials tested. The details of the electrolyte comparison are discussed below.

There is about an order of magnitude increase in the conductivity when going from the phosphoric acid solution to the EAN for both materials tested. The most likely reason for the dramatic change in conductivity when going from the phosphoric acid solution to EAN is that there is an increase in the ion concentration in the polymer when using EAN compared with the phosphoric acid solution. Ion concentration is fundamentally directly related to conductivity.¹ Some electrolyte uptake measurements on the polymer materials show that there is a difference in the amount of liquid uptake when comparing the phosphoric acid solution and the EAN, with the results seen in Table III. In addition to the phosphoric acid solution uptake being significantly lower than the EAN uptake, the phosphoric acid had to be diluted from its original form because it was more corrosive and damaging to the polymer, which will also lead to a relatively lower ion concentration. By contrast, the ionic liquid did not need to be diluted, probably because its slightly organic nature makes it more compatible with the polymer. Also, once in the polymer, the liquid electrolyte could leach out of the polymer over time, which would also decrease the ion concentration, and thus, the conductivity. Evaporation of the ionic liquid is less likely than that of the phosphoric acid solution because of its better possible association with the polymer from interaction of its hydrophobic components, in addition to its low vapor pressure.^{2,89} Overall, the ionic liquid incorporation is expected to yield a higher ion concentration in the polymer, and the data support this claim.

Structure, Ionic Liquid Uptake, and Conductivity of Ionic Liquid-Doped Polymers

By understanding composition, structure, and conductivity, the link between polymer-ionic liquid interactions and properties

can be determined. Our hypothesis is that changes in material composition will lead to changes in material structure that will likely correspond to changes in conductivity. The structure was controlled by changing the aromatic monomers, thus manipulating the rigidity and free volume of the polymer. The rigidity and free volume were thought to be important factors because previous literature has shown that confinement from rigid crystallites in Nafion has been shown to influence conductivity.⁹⁰ In addition, the nature and confinement of ionic pathways in block copolymers have been shown to also impact conductivity quite significantly.^{4,91}

Impact of Changing Aromatic Dianhydride. One way to tailor the properties of the polymer is to change the identity of the aromatic dianhydride. The 6FDA-AP6F and ODP-AP6F families can be compared to assess the influence of different dianhydride units, and the SAXS results for the undoped polymer structures can be seen in Figure 4. The ODP material shows a shoulder that is consistent with randomly distributed PEG domains in the polymer, S_{PEGOF} which corresponds to a PEG correlation length of 0.9 nm or a radius of 1.6 nm. In addition to S_{PEGOF} a broad peak is present that is attributed to aromatic polyimide ordering, P_{aOF} with a spacing value of 15.3 nm ($q = 0.41 \text{ nm}^{-1}$). P_{aOF} is believed to be due to the spacing between regions of relatively well-ordered polymer chains involving the less bulky ODP units. The 6FDA material shows only a single feature, a shoulder consistent with randomly distributed PEG domains, S_{PEGFB} with a correlation length of 0.9 nm, corresponding to a radius of 1.6 nm. The 6FDA system appears to have a more defined shoulder than the ODP case but it is difficult to assess whether this is truly related to the PEG-PI phase definition because P_{aOF} could merely be convoluting S_{PEGOF} .

There are relatively few structural features for these two materials in the undoped state. The only detectable structural difference between these two polyimides is the presence of P_{aOF} in only the ODP material. This trend is expected based on the lack of structural features seen in previously studied fluorinated

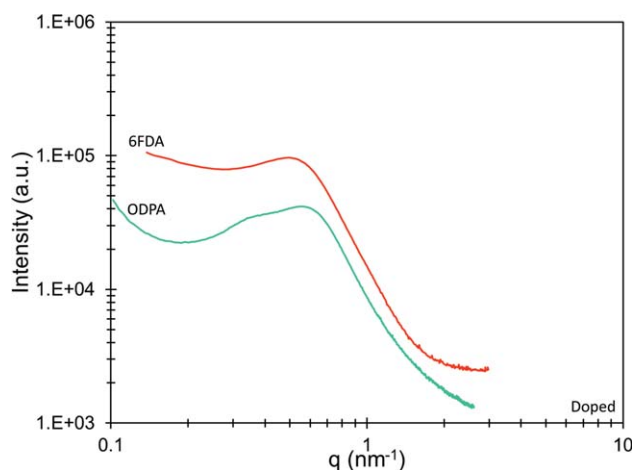


Figure 5. SAXS signatures of 6FDA-AP6F-6FDA-PEG1500 (50%) EAN and ODP-AP6F-ODPA-PEG1500 (50%) EAN materials. [Color figure can be viewed in the online issue, which is available at wileyonlinelibrary.com.]

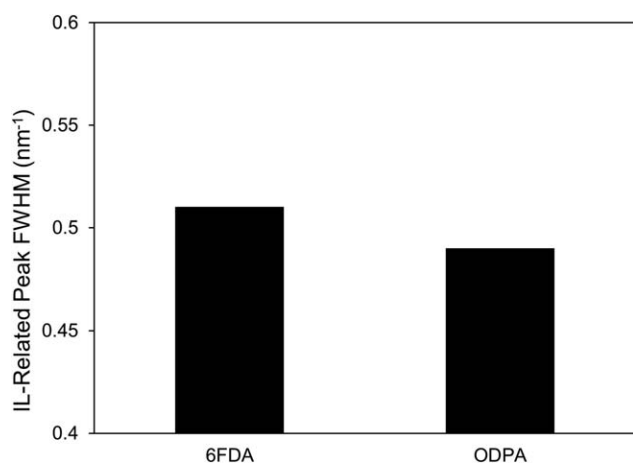


Figure 6. The FWHM of the IL-related peaks for 6FDA-AP6F-6FDA-PEG1500 (50%) EAN and ODPa-AP6F-ODPA-PEG1500 (50%) EAN materials.

polyimides and possible aromatic interaction and order generally seen in nonfluorinated polyimides.^{92–94} Both systems show shoulders that are essentially identical in size and are similar in size to PEG domains found in previously studied PEG-imide systems.^{95,96} The 6FDA system is expected to have less rigidity owing to a lack of order from closely packed or well-aligned dianhydride polymer segments based on changes in rigidity seen in other aromatic polyimides with varying levels of order.^{97–101}

There are noticeable changes in polymer structure when comparing the undoped and doped polymer systems in both of these families. The SAXS signatures of the ionic liquid-doped polymers can be seen in Figure 5. The ODPa material-doped structure shows a feature, F_{aOF} at an estimated spacing value at 15.0 nm ($q = 0.42 \text{ nm}^{-1}$), likely the remnants of P_{aOF} in the undoped polymer, and a peak, $P_{PEGILOF}$, with a spacing value of 11.6 nm ($q = 0.54 \text{ nm}^{-1}$). The 6FDA material doped structure shows a single peak, $P_{PEGILFF}$ with a spacing value of 13.4 nm ($q = 0.47 \text{ nm}^{-1}$) and is relatively broad in shape.

Both doped material structures show the presence of a peak that is attributed to a spacing between ionic-liquid-doped PEG domains. Overall, the evidence of structural changes in these polyimides upon doping is similar to changes that have occurred for ionic liquid-incorporated block copolymer systems studied before in terms of transitioning from a disordered to an ordered state.^{4,26,27,102} Previous studies have also shown that ionic liquids tend to prefer to interact with PEG as opposed to more aromatic polymers.² This evidence from previous literature supports the hypothesis that the new peak seen in both systems is related to a spacing between ionic-liquid-doped PEG domains. The ODPa polymer system also shows the weak feature, F_{aOF} , related to the polyimide order.

Although the overall structural differences are subtle, the regularity of the ether-containing dianhydride is expected to increase rigidity even when weakly present to some extent because rigidity and molecular order have been shown to correlate in previously studied polyimide systems.^{98,99,103,104} P_{aOF} loses almost all prominence once the polymer is doped and transforms into

F_{aOF} , meaning that the rigidity associated with the ether-containing dianhydride is expected to impede the polymer motion and transport only to a certain extent.

The shape of the $P_{PEGILOF}$ suggests that the spacing and regularity of the ionic liquid-doped domains might be more defined in the ODPa case. This can be more directly quantified by comparing the ionic liquid-related peak FWHM in both materials, which can be seen in Figure 6. The FWHM or relative broadness of the peak in the ODPa case is slightly smaller than that of the peak in the 6FDA case. A smaller FWHM suggests less broadness and relatively more definition in the feature likely due to more defined boundaries between phases. The IL-doped domains are possibly more defined because the aromatic regularity, likely due to the ODPa units, may provide better boundaries and order in the material.

To compare the materials further, the ionic liquid uptake was measured and recorded, and the comparison can be seen in Table IV. The ionic liquid uptake is higher for the 6FDA material as opposed to the ODPa material. Nevertheless, both values of ionic liquid uptake are on the same order of magnitude and are high in value.

The more bulky fluorinated dianhydride is expected to have more free volume and more mobility than the ether-containing dianhydride based on previous work studying polyimides.^{92,94,98,99} The additional free volume and mobility could lead to a higher possible ionic liquid uptake. The expected trend is supported by the exact values seen in the ionic liquid uptake data. The possibility for the ionic liquid to migrate into the aromatic polyimide phase is higher in the 6FDA system due to this increase in free volume. The higher ionic liquid uptake may also be because the dianhydride units are disordered as opposed to interacting or aligned. The ionic liquid-polymer boundary quality expected from the ionic liquid uptake amount in the material could explain the differences in the $P_{PEGILOF}$ and $P_{PEGILFF}$ broadness.

The conductivity results due to varying the dianhydride were also compared and can be seen in Figure 7. The conductivity generally increases with temperature for both polymers, as expected based on diffusion principles with an estimated activation energy on the order of 11–13 kJ/mol.¹ These activation energy values are in relatively good agreement with those found for PEG-poly(methacrylate) systems doped with acetic acid, which ranged from 5 to 30 kJ/mol.¹⁰⁵ The conductivity of the 6FDA material is slightly higher on average than that of the ODPa material, by about 15%, which is not very significant. Overall, the conductivity ranges indicated by the error bars representing ± 1 SD are quite similar.

Table IV. Ionic Liquid Uptake Values of 6FDA-AP6F-6FDA-PEG1500 (50%) EAN and ODPa-AP6F-ODPA-PEG1500 (50%) EAN Materials

Material	Ionic liquid	Uptake (%)
ODPA-AP6F-ODPA-PEG1500 (50%) EAN	EAN	149
6FDA-AP6F-6FDA-PEG1500 (50%) EAN	EAN	203

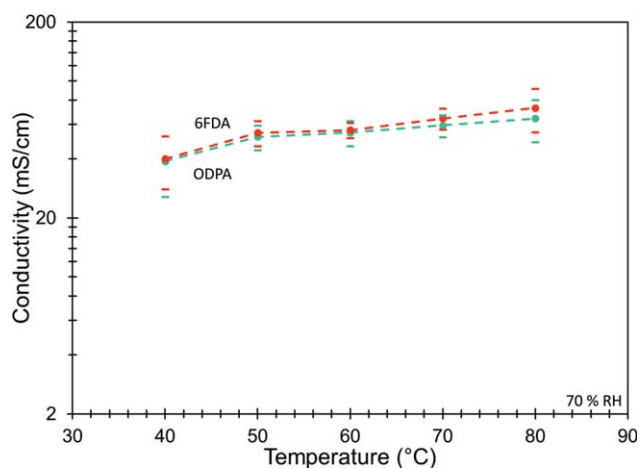


Figure 7. Conductivity of 6FDA-AP6F-6FDA-PEG1500 (50%) EAN and ODP-AP6F-ODPA-PEG1500 (50%) EAN materials at 70% RH. [Color figure can be viewed in the online issue, which is available at wileyonlinelibrary.com.]

The average conductivity behavior seen correlates with the ionic liquid uptake and expected free volume and flexibility of the two materials. The 6FDA system has more conformational freedom and volume; thus, the ions are likely to have more freedom to move. However, the conductivity differences between the two systems are not very significant despite the differences in ionic liquid uptake. F_{aOF} is only weakly present once the materials are doped meaning that rigidity imparted to the system from this component will be minimized. Some of the expected performance increase due to the decrease in rigidity of the 6FDA case could be counterbalanced by the less defined ordering or phase boundaries of the ionic liquid-doped domains, as indicated by the broadness of $P_{PEGILFF}$.

This decrease in ionic domain ordering definition could create more tortuosity or poorly defined phase boundaries that might impede the conductivity which would be consistent with effects seen and modeled in block copolymers with pathway and boundary variations. Generally, more defined boundaries and less tortuous pathways result in better conductivity.^{4,91} The minimization of the imide order upon doping and the possibly less-well-defined ionic pathways for the 6FDA material may both explain why the increase in conductivity from the fluorinated dianhydride is not very significant. Changing the dianhydride has a relatively minor effect on overall conductivity despite differences in ionic liquid uptake. The findings may be due to the fact that overall, structural differences are minimized once the ionic liquid is incorporated into these polymers and ionic liquid uptake is high for both polymers.

Impact of Changing Aromatic Diamine. The previous comparison has shown that differences in dianhydride can result in variations in aromatic structure as well as ionic liquid-related phases. Another way to possibly influence the polymer-ionic liquid interaction and ultimately the properties of these materials is to change the aromatic diamine. The results of changing the aromatic diamine on the undoped polymer structure can be seen in Figure 8. Both materials show a shoulder consistent with ran-

domly distributed PEG domains, S_{PEGFF} and S_{PEGFO} , corresponding to a correlation length size of 0.9 nm and an effective radius of 1.6 nm. The PDODA system shows evidence of a weak feature, F_{aFO} , corresponding to a spacing value of 2.2 nm ($q = 2.9 \text{ nm}^{-1}$). F_{aFO} is most likely related to the regularity of the aromatic structure, more specifically, the PDODA diamine. S_{PEGFF} is somewhat more well-defined than S_{PEGFO} , although it is difficult to state whether this difference is significant.

The undoped polymers appear very similar to each other with regard to structure. Both systems show shoulders consistent with random PEG domains with identical correlation length, with the PDODA system showing possible weaker phase separation that could be due to miscibility changes or steric interference from polyimide order. The size of the PEG domains is similar to PEG domains in PEG-imide systems previously studied.^{95,96}

F_{aFO} in the PDODA family is the only significant difference between the structures of these two polyimide families. The feature is only present when the PDODA diamine unit is used in the synthesis, lending support for the theory that the feature seen in the current system is related to the regularity or order of the PDODA portion of the aromatic repeat unit.

Similar features to this one have been seen in previously studied aromatic polyimides, which are also believed to be due to regularity of the aromatic repeat unit.¹⁰⁶⁻¹⁰⁸ Some minimal amount of rigidity and strength is expected to arise owing to this regularity of the aromatic repeat unit. Previous work on aromatic polyimides has shown that variations in rigidity can result from changes in aromatic monomers and the varying amount of order associated with them.^{98,99}

The structures of the EAN-doped polymers were also characterized, and the results can be seen in Figure 9. The two polymer systems qualitatively look similar to each other. Each has a peak related to the ionic liquid incorporation, $P_{PEGILFF}$ and $P_{PEGILFO}$; more specifically, this peak is believed to correspond to the spacing associated with the ionic liquid-doped PEG phase of

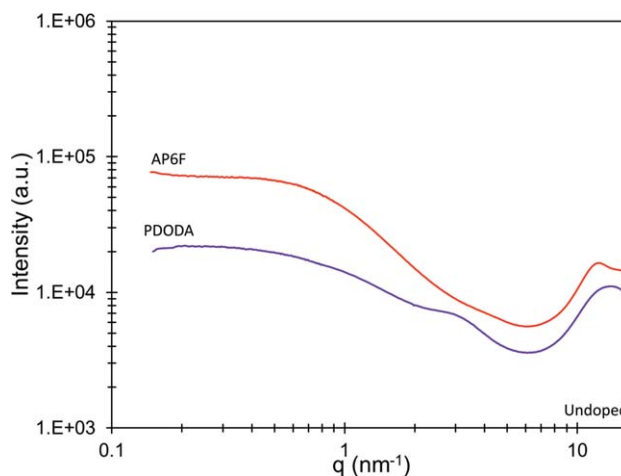


Figure 8. SAXS signatures of 6FDA-AP6F-6FDA-PEG1500 (50%) and 6FDA-PDODA-6FDA-PEG1500 (50%) polymers. [Color figure can be viewed in the online issue, which is available at wileyonlinelibrary.com.]

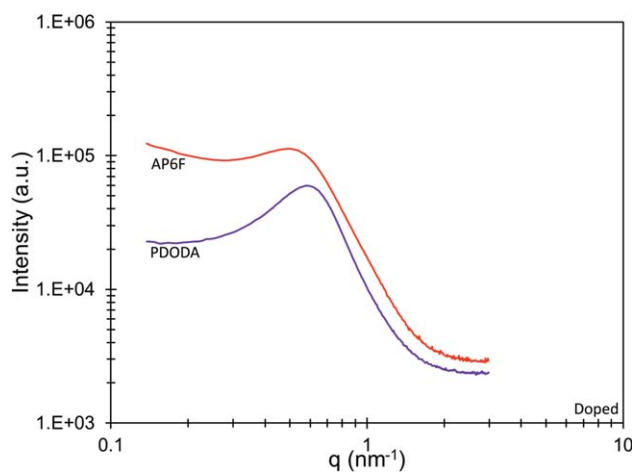


Figure 9. SAXS signatures of 6FDA-AP6F-6FDA-PEG1500 (50%) EAN and 6FDA-PDODA-6FDA-PEG1500 (50%) EAN materials. [Color figure can be viewed in the online issue, which is available at wileyonlinelibrary.com.]

the material. As a recap, in the AP6F system seen previously, P_{PEGILFF} is broad and somewhat less well defined with a spacing value of 13.4 nm ($q = 0.47 \text{ nm}^{-1}$). In the PDODA system, P_{PEGILFO} is more well defined with a spacing value of 11.0 nm ($q = 0.57 \text{ nm}^{-1}$). In the doped polymer structures there is no clear evidence of F_{aFO} seen in the undoped PDODA structure.

The doped polymer structures of these two systems look similar with the single peak attributed to the spacing from the ordering of the ionic liquid-doped PEG phase that is similar to disorder to order structural rearrangements seen in ionic liquid-incorporated block copolymer systems studied previously.^{4,26,27,102} Overall, the only structural difference is the relative broadness and definition of the peak, with the PDODA system showing more definition. The differences in these features can be directly compared and quantified by examining their FWHM values which can be seen in Figure 10. In the AP6F material the peak has a much larger FWHM than in the PDODA case, thereby providing quantitative evidence of the

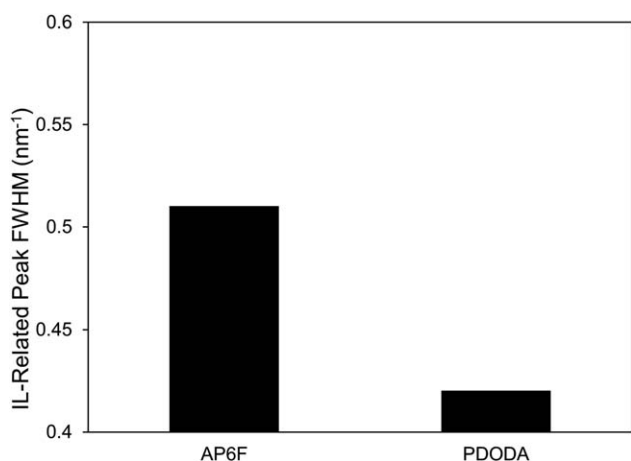


Figure 10. The FWHM of the IL-related peaks for the 6FDA-AP6F-6FDA-PEG1500 (50%) EAN and 6FDA-PDODA-6FDA-PEG1500 (50%) EAN materials.

less broad, more defined phases present in the PDODA material.

To further compare the materials, the ionic liquid uptake measurements were quantitatively assessed and the results can be seen in Table V. Although both ionic liquid uptake amounts are on the same order of magnitude, the AP6F system has higher ionic liquid uptake when compared with the PDODA material. The more defined P_{PEGILFO} when compared with P_{PEGILFF} is present in the system with less ionic liquid uptake.

The AP6F system has higher ionic liquid uptake but less P_{PEGILFO} definition, which may appear counterintuitive. The more defined P_{PEGILFO} may indicate better definition in the ordering of the doped PEG domains and thus more defined ionic conduction pathways. Although the presence of F_{aFO} cannot be seen in the doped polymer structure, the diamine identity could contribute to a difference in free volume and ring orientation, which might impact how likely it is that the ionic liquid will intercalate into the aromatic polyimide phase. Free volume changes have been seen with various aromatic units in previously studied aromatic polyimides and can impact transport properties and motion, which provides some qualitative evidence for the ionic liquid intercalation hypothesis.^{98,99,103,104} The ionic liquid uptake results also suggest less possible intercalation of the ionic liquid into the aromatic phase in the PDODA material from an absolute amount of ionic liquid perspective.

From previously presented undoped polymer structural datasets as well as previous studies on aromatic polyimides, the PDODA system would appear to have more rigidity based on the finding that those polyimides with order tend to show an increase in rigidity.^{93,97-101} The fact that F_{aFO} is not present in the doped structure suggests that there will be no significant differences in rigidity between the two doped polymer systems.

Although the data show that the rigidity differences in these polymers may be negligible, the lower ionic liquid uptake suggests that the PDODA system will result in lower conductivity, while the better definition of the P_{PEGILFO} when compared with P_{PEGILFF} suggests that the conductivity may be higher because previous evidence in ionic liquid-incorporated polymer electrolytes suggests better conductivity for more well-defined pathways.^{2,4} Thus, there are competing factors that come into play in this set of materials.

The conductivity of these two materials doped with EAN was also compared at 70% RH, with the results given in Figure 11. The conductivity increases as temperature increases for both polymer systems, as expected based on diffusion behavior with an estimated activation energy on the order of 8–13 kJ/mol,

Table V. Ionic Liquid Uptake Values of 6FDA-AP6F-6FDA-PEG1500 (50%) EAN and 6FDA-PDODA-6FDA-PEG1500 (50%) EAN Materials

Material	Ionic liquid	Uptake (%)
6FDA-AP6F-6FDA-PEG1500 (50%) EAN	EAN	203
6FDA-PDODA-6FDA-PEG1500 (50%) EAN	EAN	154

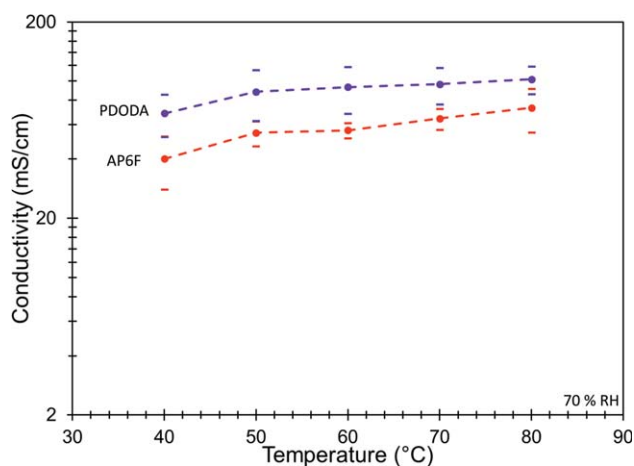


Figure 11. Conductivity of 6FDA-AP6F-6FDA-PEG1500 (50%) EAN and 6FDA-PDODA-6FDA-PEG1500 (50%) EAN materials at 70% RH. [Color figure can be viewed in the online issue, which is available at wileyonlinelibrary.com.]

which are in relatively good agreement with those found for PEG-poly(methacrylate) systems doped with acetic acid ranging from 5 to 30 kJ/mol.^{1,105} The conductivity of the PDODA polymer system is about 28% higher than the AP6F system and the difference appears significant.

Overall, the conductivity of the PDODA system was found to be higher than the AP6F system. The narrower nature of the P_{PEGILFO} likely from better definition of the ionic liquid-related structure appears to be dominant over the ionic liquid uptake differences, likely because the ionic liquid uptake values are fairly high for both systems. The better defined ionic pathway structure outweighs the differences in ionic content for this material set in determining performance. Structural definition and nature of ionic pathways through a polymer material are known to impact conductivity in other polymer electrolyte materials as well.^{4,91} The better defined ionic pathways most likely result from ionic liquid distribution differences in the aromatic phase of these materials stemming from free volume effects. The conductivity in this material comparison correlates with the trend of expected free volume and ionic pathway definition.

The impact of changing aromatic diamine is moderately significant leading to a 28% change in conductivity. The change in diamine leads to differences in the doped polymer structure definition which is likely related to the ionic liquid pathways. Ultimately, the structural definition in these specific materials changes the performance significantly, likely from free volume dissimilarities, as there is essentially no indication of differences in rigidity for the doped polymers.

CONCLUSIONS

In this particular polymer system, changes in liquid electrolyte impact conductivity and changes in aromatic dianhydride and aromatic diamine affect the polymer rigidity and free volume. These factors ultimately impacted the polymer-ionic liquid phase definition, which can have subtle to moderate impacts on

performance. The work has shown that a variety of different material factors can affect the structure and properties of these materials and that often different factors may work in concert or in an antagonistic manner. The composition, structure, and properties in these materials are seen to be multifaceted and interconnected, not always in linear or expected ways.

When switching from the ODPA dianhydride to the 6FDA dianhydride using the AP6F diamine for 50 wt % PEG 1500, the conductivity increases on average by only 15%. The larger free volume and bulky nature of the 6FDA dianhydride prevents any ordered aromatic structural components, which leaves the polymer less rigid and more able to move, uptake ionic liquid, and conduct ions. The effect is minimal because the structural rigidity differences of these two polymers once doped are relatively small and the ionic pathway boundaries may be less defined for the 6FDA system.

When the diamine is changed from AP6F to PDODA while using the 6FDA dianhydride for 50 wt % PEG 1500, there is an increase in conductivity by 28%. This increase in conductivity is likely related to the more planar, less bulky PDODA system producing more well-defined doped polymer ionic pathway phase boundaries, which may result in better ion conduction pathways through the material. There are competing factors with this material comparison, but ultimately a significant change in the performance is seen.

Our initial evaluations have shown that the properties of these materials can be engineered through compositional and structural changes. The performance of the current systems is high enough to potentially warrant further studies. Other properties necessary for an optimal PEM including mechanical strength and hydrogen and oxygen permeability should be evaluated to determine if these materials have the potential to be in a commercial fuel cell. One advantage of this system is that a set of polymer matrices were created with different properties that are able to be incorporated with a liquid ion source. By changing the type of ion source, these materials could potentially be used for other applications including battery electrolytes, gas separation membranes, or actuators. This set of material enables flexibility and tuning of properties.

ACKNOWLEDGMENTS

This work was funded by the National Defense Science and Engineering Graduate Fellowship and the Precourt Institute for Energy. This work would not have been possible without the assistance of Thomas Jaramillo, Andrew Spakowitz, John Pople, Sean Brennan, Christopher Tassone, Steve He, Desmond Ng, Shifan Mao, and Zhebo Chen.

REFERENCES

- O'Hayre, R.; Cha, S.-W.; Colella, W.; Prinz, F. B. *Fuel Cell Fundamentals*; John Wiley & Sons, Inc.: Hoboken, New Jersey, 2009.
- Park, M. J.; Choi, I.; Hong, J.; Kim, O. J. *J. Appl. Polym. Sci.* 2013, 129, 2363.

3. Ye, Y. S.; Rick, J.; Hwang, B. J. *J. Mater. Chem. A* **2013**, *1*, 2719.
4. Young, W. S.; Kuan, W. F.; Epps, T. H. *J. Polym. Sci. Part B: Polym. Phys.* **2013**, *52*, 1.
5. Marcos-Fernández, A.; Tena, A.; Lozano, A. E.; de la Campa, J. G.; de Abajo, J.; Palacio, L.; Prádanos, P.; Hernández, A. *Eur. Polym. J.* **2010**, *46*, 2352.
6. Muellerleile, J. T.; Risch, B. G.; Rodrigues, D. E.; Garth, L. *Techniques* **1993**, *34*, 789.
7. Pandiyan, S.; Brown, D.; Van Der Vegt, N. F. A.; Neyertz, S. *J. Polym. Sci. Part B: Polym. Phys.* **2009**, *47*, 1166.
8. Russell, T. P. *J. Polym. Sci. Part B: Polym. Phys.* **1984**, *22*, 1105.
9. Russell, T. P.; Brown, H. R. *J. Polym. Sci. Part B: Polym. Phys.* **1987**, *25*, 1129.
10. Saraf, R. F. *Polym. Eng. Sci.* **1997**, *37*, 1195.
11. Tena, A.; Lozano, A. E.; Palacio, L.; Marcos-Fernández, A.; Prádanos, P.; de Abajo, J.; Hernández, A. *Int. J. Greenh. Gas Control* **2013**, *12*, 146.
12. Tena, A.; de la Viuda, M.; Palacio, L.; Prádanos, P.; Marcos-Fernández, A.; Lozano, A. E.; Hernández, A. *J. Membr. Sci.* **2014**, *453*, 27.
13. Tena, A.; Marcos-Fernández, A.; Palacio, L.; Cuadrado, P.; Prádanos, P.; de Abajo, J.; Lozano, A. E.; Hernández, A. *Ind. Eng. Chem. Res.* **2012**, *51*, 3766.
14. Tena, A.; Marcos-Fernández, A.; Lozano, A. E.; de la Campa, J. G.; de Abajo, J.; Palacio, L.; Prádanos, P.; Hernández, A. *J. Membr. Sci.* **2012**, *387–388*, 54.
15. Tena, A.; Marcos-Fernández, A.; Palacio, L.; Prádanos, P.; Lozano, A. E.; de Abajo, J.; Hernández, A. *J. Membr. Sci.* **2013**, *434*, 26.
16. Armand, M.; Endres, F.; MacFarlane, D. R.; Ohno, H.; Scrosati, B. *Nat. Mater.* **2009**, *8*, 621.
17. Sekhon, S. S.; Lalia, B. S.; Park, J.-S.; Kim, C.-S.; Yamada, K. *J. Mater. Chem.* **2006**, *16*, 2256.
18. Sekhon, S. S.; Park, J.-S.; Cho, E.; Yoon, Y.-G.; Kim, C.-S.; Lee, W.-Y. *Macromolecules* **2009**, *42*, 2054.
19. Wang, S. W.; Liu, W.; Colby, R. H. *Chem. Mater.* **2011**, *23*, 1862.
20. Mistry, M. K.; Subianto, S.; Choudhury, N. R.; Dutta, N. K. *Langmuir* **2009**, *25*, 9240.
21. Kumar, M.; Venkatnathan, A. *J. Phys. Chem. B* **2013**, *117*, 14449.
22. Gao, J.; Guo, Y.; Wu, B.; Qi, L.; Li, B.; Liu, J.; Wang, Z.; Liu, W.; Gu, J.; Zou, Z. *J. Power Sources* **2014**, *251*, 432.
23. Doyle, M.; Choi, S. K.; Proulx, G. *J. Electrochem. Soc.* **2000**, *147*, 34.
24. Susan, M. A. B. H.; Kaneko, T.; Noda, A.; Watanabe, M. *J. Am. Chem. Soc.* **2005**, *127*, 4976.
25. Vázquez, M. I.; Romero, V.; Fontàs, C.; Anticó, E.; Benavente, J. *J. Membr. Sci.* **2014**, *455*, 312.
26. Gwee, L.; Choi, J. H.; Winey, K. I.; Elabd, Y. A. *Polymer (Guildf)*. **2010**, *51*, 5516.
27. Kim, S. Y.; Kim, S.; Park, M. *J. Nat. Commun.* **2010**, *1*, 1.
28. Noro, A.; Matsushima, S.; He, X.; Hayashi, M.; Matsushita, Y. *Macromolecules* **2013**, *46*, 8304.
29. Si, Z.; Gu, F.; Guo, J.; Yan, F. *J. Polym. Sci. Part B: Polym. Phys.* **2013**, *51*, 1311.
30. Vidal, F.; Plesse, C.; Palaprat, G.; Juger, J.; Gauthier, C.; Pelletier, J.-M.; Masenelli-Varlot, K.; Chevrot, C.; Teyssié, D. *Eur. Polym. J.* **2013**, *49*, 2670.
31. Wang, Y.-P.; Gao, X.-H.; Chen, J.-C.; Li, Z.-W.; Li, C.-L.; Zhang, S.-C. *J. Appl. Polym. Sci.* **2009**, *113*, 2492.
32. Kim, J.-K.; Ahn, J.-H.; Jacobsson, P. *Electrochim. Acta* **2014**, *116*, 321.
33. Kim, J. K.; Niedzicki, L.; Scheers, J.; Shin, C. R.; Lim, D. H.; Wiczorek, W.; Johansson, P.; Ahn, J. H.; Matic, A.; Jacobsson, P. *J. Power Sources* **2013**, *224*, 93.
34. Li, H.; Jiang, F.; Di, Z.; Gu, J. *Electrochim. Acta* **2012**, *59*, 86.
35. Li, M.; Yang, L.; Fang, S.; Dong, S.; Jin, Y.; Hirano, S.-I.; Tachibana, K. *J. Power Sources* **2011**, *196*, 6502.
36. Nath, A. K.; Kumar, A. *Electrochim. Acta* **2014**, *129*, 177.
37. Pandey, G. P.; Hashmi, S. A. *J. Power Sources* **2013**, *243*, 211.
38. Suleman, M.; Kumar, Y.; Hashmi, S. A. *J. Phys. Chem. B* **2013**, *117*, 7436.
39. Yang, P. X.; Liu, L.; Li, L. B.; Hou, J.; Xu, Y. P.; Ren, X.; An, M. Z.; Li, N. *Electrochim. Acta* **2014**, *115*, 454.
40. Yeon, S. H.; Kim, K. S.; Choi, S.; Cha, J. H.; Lee, H. *J. Phys. Chem. B* **2005**, *109*, 17928.
41. Zalewska, A.; Dumińska, J.; Langwald, N.; Syzdek, J.; Zawadzki, M. *Electrochim. Acta* **2014**, *121*, 337.
42. Ma, H.; Chen, X.; Hsiao, B. S.; Chu, B. *Polymer (Guildf)*. **2014**, *55*, 160.
43. Seki, S.; Susan, M. A. B. H.; Kaneko, T.; Tokuda, H.; Noda, A. *J. Phys. Chem. B* **2005**, *109*, 3886.
44. Frank-Finney, R. J.; Bradley, L. C.; Gupta, M. *Macromolecules* **2013**, *46*, 6852.
45. Reddy, B. N.; Deepa, M. *Polymer (Guildf)*. **2013**, *54*, 5801.
46. Virgili, J. M.; Hoarfrost, M. L.; Segalman, R. A. *Macromolecules* **2010**, *43*, 5417.
47. Parveen, N.; Schönhoff, M. *Macromolecules* **2013**, *46*, 7880.
48. He, Y.; Lodge, T. P. *Chem. Commun. (Camb)*. **2007**, 2732.
49. He, Y.; Boswell, P. G.; Bühlmann, P.; Lodge, T. P. *J. Phys. Chem. B* **2007**, *111*, 4645.
50. He, P.; Chen, B.; Wang, Y.; Xie, Z.; Dong, F. *Electrochim. Acta* **2013**, *111*, 108.
51. Debeljuh, N. J.; Sutti, A.; Barrow, C. J.; Byrne, N. *J. Phys. Chem. B* **2013**, *117*, 8430.
52. Xiong, S.; Xie, K.; Blomberg, E.; Jacobsson, P.; Matic, A. *J. Power Sources* **2014**, *252*, 150.
53. Xiang, J.; Wu, F.; Chen, R.; Li, L.; Yu, H. *J. Power Sources* **2013**, *233*, 115.
54. Deligöz, H.; Yilmazoğlu, M. *J. Power Sources* **2011**, *196*, 3496.

55. Deligöz, H.; Yilmazoğlu, M.; Yilmaztürk, S.; Şahin, Y.; Ulutaş, K. *Polym. Adv. Technol.* **2012**, *23*, 1156.
56. Kanehashi, S.; Kishida, M.; Kidesaki, T.; Shindo, R.; Sato, S.; Miyakoshi, T.; Nagai, K. *J. Membr. Sci.* **2013**, *430*, 211.
57. Li, P.; Coleman, M. R. *Eur. Polym. J.* **2013**, *49*, 482.
58. Liang, L.; Gan, Q.; Nancarrow, P. J. *Membr. Sci.* **2014**, *450*, 407.
59. Akbarian-Feizi, L.; Mehdipour-Ataei, S.; Yeganeh, H. J. *Appl. Polym. Sci.* **2012**, *124*, 1981.
60. Bennett, M. D.; Leo, D. J.; Wilkes, G. L.; Beyer, F. L.; Pechar, T. W. *Polymer (Guildf)*. **2006**, *47*, 6782.
61. Brown, R. H.; Duncan, A. J.; Choi, J.-H.; Park, J. K.; Wu, T.; Leo, D. J.; Winey, K. I.; Moore, R. B.; Long, T. E. *Macromolecules* **2010**, *43*, 790.
62. Che, Q.; He, R.; Yang, J.; Feng, L.; Savinell, R. F. *Electrochem. Commun.* **2010**, *12*, 647.
63. Chen, B.-K.; Wu, T.-Y.; Kuo, C.-W.; Peng, Y.-C.; Shih, I.-C.; Hao, L. Sun, I.-W. *Int. J. Hydrogen Energy* **2013**, *38*, 11321.
64. Imaizumi, S.; Ohtsuki, Y.; Yasuda, T.; Kokubo, H.; Watanabe, M. *ACS Appl. Mater. Interfaces* **2013**, *5*, 6307.
65. Kim, J.-K.; Matic, A.; Ahn, J.-H.; Jacobsson, P. J. *Power Sources* **2010**, *195*, 7639.
66. Kim, O.; Kim, Y. S.; Ahn, H.; Kim, C. W.; Rhee, Y. M.; Park, M. J. *Macromolecules* **2012**, *45*, 8702.
67. Kim, S. Y.; Yoon, E.; Joo, T.; Park, M. J. *Macromolecules* **2011**, *44*, 5289.
68. Lee, S. Y.; Ogawa, A.; Kanno, M.; Nakamoto, H.; Yasuda, T.; Watanabe, M. *J. Am. Chem. Soc.* **2010**, *132*, 9764.
69. Lee, S.-Y.; Yasuda, T.; Watanabe, M. *J. Power Sources* **2010**, *195*, 5909.
70. Mistri, E. A.; Mohanty, A. K.; Banerjee, S. *J. Membr. Sci.* **2012**, *411–412*, 117.
71. Yasuda, T.; Nakamura, S.-I.; Honda, Y.; Kinugawa, K.; Lee, S.-Y.; Watanabe, M. *ACS Appl. Mater. Interfaces* **2012**, *4*, 1783.
72. Yasuda, T.; Watanabe, M. *MRS Bull.* **2013**, *38*, 560.
73. Diddens, D.; Heuer, A. *J. Phys. Chem. B* **2014**, *118*, 1113.
74. Mondal, J.; Choi, E.; Yethiraj, A. *Macromolecules* **2014**, *47*, 438.
75. Xue, F.; Jiang, S. *RSC Adv.* **2013**, *3*, 23895.
76. Hammouda, B. The SANS Toolbox; NIST Center for Neutron Research. Gaithersburg, Maryland, **1995**.
77. Jung, C.; Jikei, M.; Kakimoto, M. *Opt. Soc. Am. B* **1998**, *15*, 471.
78. Li, Q.; Yang, X.; Chen, W.; Yi, C.; Xu, Z. *Macromol. Symp.* **2008**, *261*, 148.
79. Liu, P. *Iran. Polym. J.* **2005**, *14*, 968.
80. Yang, J.; Lee, M. A. *Macromol. Res.* **2004**, *12*, 263.
81. Chen, H.; Xiao, Y.; Chung, T.-S. *Polymer (Guildf)*. **2010**, *51*, 4077.
82. Huertas, R. M.; Doherty, C. M.; Hill, A. J.; Lozano, A. E.; de Abajo, J.; de la Campa, J. G.; Maya, E. M. *J. Membr. Sci.* **2012**, *409–410*, 200.
83. Maya, E. M.; Muñoz, D. M.; de la Campa, J. G.; de Abajo, J.; Lozano, Á. E. *Desalination* **2006**, *199*, 188.
84. Maya, E. M.; Munoz, D. M.; Lozano, A. E.; De Abajo, J.; De; La Campa, J. G. *J. Polym. Sci. Part A: Polym. Chem.* **2008**, *46*, 8170.
85. Vincent, C. A. *Prog. Solid State Chem.* **1987**, *17*, 145.
86. Wright, P. V. *Electrochim. Acta* **1998**, *43*, 1137.
87. Kreuer, K. D. *Chem. Mater.* **2014**, *26*, 361.
88. Rozière, J.; Jones, D. J. *Annu. Rev. Mater. Res.* **2003**, *33*, 503.
89. Park, N. K.; Bae, Y. C. *J. Polym. Sci. Part B: Polym. Phys.* **2010**, *48*, 212.
90. Liu, J.; Suraweera, N.; Keffer, D. J.; Cui, S.; Paddison, S. J. *J. Phys. Chem. C* **2010**, *114*, 11279.
91. Ganesan, V.; Pyramitsyn, V.; Bertoni, C.; Shah, M. *ACS Macro Lett.* **2012**, *1*, 513.
92. Choi, S.; Kim, Y.; Kim, I.; Ha, C. *J. Appl. Polym. Sci.* **2007**, *103*, 2507.
93. Fu, Q.; Livengood, B. P.; Shen, C. C.; Lin, F. L.; Harris, F. W.; Cheng, S. Z. D.; Hsiao, B. S.; Yeh, F. *Macromol. Chem. Phys.* **1998**, *199*, 1107.
94. Morikawa, A.; Miyata, F.; Nishimura, J. *High Perform. Polym.* **2012**, *24*, 783.
95. Costa, G.; Eastmond, G. C.; Fairclough, J. P. A.; Paprotny, J.; Ryan, A. J.; Stagnaro, P. *Macromolecules* **2008**, *41*, 1034.
96. Kricheldorf, H. R.; Schwarz, G.; Berghahn, M.; de Abajo, J.; de la Campa, J. G. *Macromolecules* **1994**, *27*, 2540.
97. Huo, P. P.; Friler, J. B.; Cebe, P. *Polymer (Guildf)*. **1993**, *34*, 4387.
98. Lazareva, Y. N.; Vidyakin, M. N.; Alentiev, A. Y.; Yablokova, M. Y.; Kuznetsov, A. A.; Ronova, I. A. *Polym. Sci. Ser. A* **2009**, *51*, 1068.
99. Low, B. T.; Xiao, Y.; Chung, T. S. *Polymer (Guildf)*. **2009**, *50*, 3250.
100. Ree, M.; Nunes, T. L.; Lin, J. S. *Polymer (Guildf)*. **1994**, *35*, 1148.
101. Srinivas, S.; Wilkes, G. L. *Polymer (Guildf)*. **1998**, *39*, 5839.
102. Simone, P. M.; Lodge, T. P. *ACS Appl. Mater. Interfaces* **2009**, *1*, 2812.
103. Okamoto, K.-i.; Fujii, M.; Okamoto, S.; Suzuki, H.; Tanaka, K.; Kita, H. *Macromolecules* **1995**, *28*, 6950.
104. Okamoto, K.-i.; Umeo, N.; Okamoto, S.; Tanaka, K.; Kita, H. *Chem. Lett.* **1993**, 225.
105. Qiao, J.; Yoshimoto, N.; Ishikawa, M.; Morita, M. *Electrochim. Acta* **2002**, *47*, 3441.
106. Wakita, J.; Jin, S.; Shin, T. J.; Ree, M.; Ando, S. *Macromolecules* **2010**, *43*, 1930.
107. Pan, R.; Zhou, T.; Zhang, A.; Zhao, W.; Gu, Y. *J. Polym. Sci. Part B: Polym. Phys.* **2010**, *48*, 2257.
108. Niu, H.; Huang, M.; Qi, S.; Han, E.; Tian, G.; Wang, X.; Wu, D. *Polymer (Guildf)*. **2013**, *54*, 1700.